communications physics

ARTICLE

https://doi.org/10.1038/s42005-023-01295-w OPEN

Open quantum system violates generalized Pauli constraints on quantum device

Irma Avdic [1], LeeAnn M. Sager-Smith [1] & David A. Mazziotti [1]✉

The Pauli exclusion principle governs the fundamental structure and function of fermionic systems from molecules to materials. Nonetheless, when such a fermionic system is in a pure state, it is subject to additional restrictions known as the generalized Pauli constraints (GPCs). Here we verify experimentally the violation of the GPCs for an open quantum system using data from a superconducting-qubit quantum computer. We prepare states of systems with three-to-seven qubits directly on the quantum device and measure the one-fermion reduced density matrix (1-RDM) from which we can test the GPCs. We find that the GPCs of the 1-RDM are sufficiently sensitive to detect the openness of the 3-to-7 qubit systems in the presence of a single-qubit environment. Results confirm experimentally that the openness of a many-fermion quantum system can be decoded from only a knowledge of the 1-RDM with potential applications from quantum computing and sensing to noise-assisted energy transfer.

[1] Department of Chemistry and The James Franck Institute, The University of Chicago, Chicago, IL 60637, USA. ✉email: damazz@uchicago.edu

In 1925, Pauli postulated that two identical fermions cannot occupy the same quantum state[1], a principle that has wide-ranging implications for the qualitative behavior of fermionic systems, e.g., Aufbau principle. Shortly thereafter, Dirac and Heisenberg showed that the Pauli exclusion principle is a consequence of the antisymmetry of the fermionic wave function[2,3]. As shown by Coleman in 1963[4], when the exclusion principle is applied to the occupations of the natural orbitals (eigenfunctions) of the one-electron reduced density matrix (1-RDM), it provides necessary and sufficient constraints that the 1-RDM is representable by at least one ensemble N-electron density matrix, known as ensemble N-representability conditions. In 1971, using calculations on IBM computers, Borland and Dennis discovered additional restrictions on the natural-orbital occupations, known as the generalized Pauli constraints (GPCs) or pure-state N-representability conditions[5]. While the first constraint discovered by Borland and Dennis is specific to three electrons in six orbitals—the Borland–Dennis constraint, more recently, Klyachko and Altunbulak generalized the Borland–Dennis constraint using enumerative algebraic geometry to generate inequalities that include larger numbers of particles and orbitals[6,7]. These constraints allow for a systematic interpretation of the 1-RDM behavior with applications in electronic structure theory[8–19], open quantum systems[20–22], and the foundations of quantum theory[8,11]. In addition, GPCs can be used to assess the nature of electron correlation and entanglement, which may be exploited to address aspects of quantum simulation and error-mitigation on noisy intermediate-scale quantum devices.

Recently, Smart et al. randomly prepared correlated quantum many-fermion states on the quantum computer and measured their satisfaction of the GPCs[23]. This work experimentally verified the GPCs and highlighted restrictions imposed by the GPCs on many-qubit systems in pure states. Prior to this demonstration, Chakraborty and Mazziotti postulated the sufficient condition for the openness of a many-fermion quantum system at the level of a single fermion by probing the 1-RDM's violation of GPCs[22]. These findings provided a geometric picture of a quantum system's interaction with its environment (quantum noise) based on the GPCs, and offered insight into the relationship between entanglement and openness of a quantum system. In this work, we experimentally verify the GPCs as sufficient conditions for the openness of quantum systems using a superconducting-qubit quantum computer. Specifically, we prepare quantum states of systems with three-to-seven qubits and measure occupations of their natural orbitals on quantum devices, where each qubit is treated as a site with one fermion and two separate orbitals. Quantum computation allows us to measure experimentally the orbital occupations and provide a framework for probing GPCs in open quantum systems, opening new avenues for novel approaches to quantum sensing and simulation.

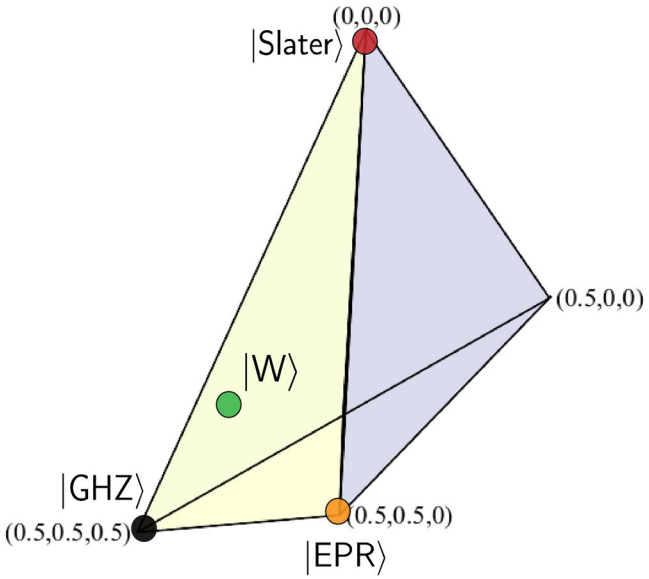

Fig. 1 Pauli polytope for three fermions in six orbitals. A convex set, known as the Pauli polytope, formed from the ordered natural occupations of the one-particle reduced density matrix (1-RDM) for three fermions in six orbitals. The sets of occupations lying inside the yellow region of the polytope, i.e., obeying the generalized Pauli constraints (GPCs), are compatible with at least one closed (pure-state) quantum system. Sets of natural occupations that lie in the blue region of the polytope, i.e., violating the GPCs, are only compatible with an open (ensemble) quantum system. The labeled points represent characteristic entangled states captured by the polytope, $|W\rangle$ $(\frac{1}{3},\frac{1}{3},\frac{1}{3})$, $|$EPR (Einstein-Podolsky-Rosen)$\rangle$ $(\frac{1}{2},\frac{1}{2},0)$, and $|$GHZ (Greenberger-Horne-Zeilinger)$\rangle$ $(\frac{1}{2},\frac{1}{2},\frac{1}{2})$, and an unentangled state $|$Slater$\rangle$ (0,0,0) for this system.

Results

Theory. Quantum computation allows for the direct preparation of quantum states and is suitable for studying highly entangled systems[24–36]. We systematically prepare quantum states of systems with three-to-seven qubits and measure eigenvalues of the one-fermion reduced density matrix (1-RDM) on the ibmq_jakarta quantum computer accessed through IBM Quantum[37]. The 1-RDM is defined by the integration of the N-fermion density matrix over the coordinates of all fermions except one

$$^1D(1;\bar{1}) = \int {}^N D(12\ldots N;\bar{1}2\ldots N)d2d3\ldots dN. \quad (1)$$

The eigenfunctions of the 1-RDM are known as the natural orbitals ϕ_i, and the eigenvalues are known as the natural orbital occupation numbers n_i. The Borland–Dennis constraints on three fermions in six orbitals, also known as GPCs or pure-state N-representability conditions of the 1-RDM, can be expressed in terms of the natural occupation numbers

$$n_5 + n_6 - n_4 \geq 0 \quad (2)$$

$$n_1 + n_6 = 1, n_2 + n_5 = 1, n_3 + n_4 = 1, \quad (3)$$

where $n_i \geq n_{i+1}$[5]. If the GPCs are satisfied, there is at least one N-qubit state which is pure. However, not every N-qubit state that satisfies the GPCs is necessarily a pure state. Therefore, the violation of the GPCs provides only a sufficient condition for determining the ensemble character, i.e., openness of the quantum system. The physical relevance of GPCs to many-fermion systems is the most prominent in cases of complete saturation (pinning) and partial saturation (quasipinning) of the constraints[8,9,13,14,38] where pinning (or quasipinning) reveals fundamental one-body symmetries (or quasi-symmetries) of the system.

In the case of three fermions in six orbitals, the ordered set of the three smallest 1-RDM eigenvalues forms a polytope, a closed convex set with flat facets, known as the Pauli polytope, shown in Fig. 1. Both the yellow and blue regions of the polytope are allowed for occupation numbers from an ensemble (open) system, but only the yellow region of the polytope is allowed for a pure-state system. The facet separating the yellow and blue regions is the first-discovered GPC—the Borland–Dennis constraint. The following key states from quantum information are labeled in the polytope: $|W\rangle$ $(\frac{1}{3},\frac{1}{3},\frac{1}{3})$[39], $|$EPR$\rangle$ $(\frac{1}{2},\frac{1}{2},0)$[40], and $|$GHZ$\rangle$ $(\frac{1}{2},\frac{1}{2},\frac{1}{2})$[41], and an unentangled state $|$Slater$\rangle$ (0,0,0) where EPR and

GHZ denote Einstein-Podolsky-Rosen and Greenberger-Horne-Zeilinger, respectively.

For four fermions in eight orbitals and five fermions in ten orbitals, there are 14 and 161 known inequalities, respectively, that define their necessary and sufficient pure-state N-representability conditions[7]. Violation of a single constraint demonstrates that the quantum system cannot be in a pure N-electron state. Here we restrict the fermions and their orbitals to form qubits. The $2N$ orbitals are paired with the occupation of each pair of orbitals being restricted to one fermion. Importantly, in this case in which the fermions are also qubits, the GPCs for N fermions in $2N$ orbitals reduce to a single inequality[42] defined as follows:

$$\sum_{i=N+2}^{r} n_i - n_{N+1} \geq 0, \tag{4}$$

where n_i are the smallest N eigenvalues for the system and r is the number of orbitals.

Each qubit on a quantum device is composed of a particle and a hole, and collectively these particles and holes obey fermion statistics. This is true even though the qubits, which are particle-hole quasi-particles, do not obey fermion statistics. Though our approach does not explicitly specify using a quantum device built from fermions, as recently proposed in Hackl et al. [43], it allows for probing the GPCs on quantum systems that follow fermion statistics by directly measuring orbital occupations on quantum computers, as supported by our previous work[23,27,28,36]. Since we are exploring a phenomenon produced as a consequence of the qubit particle-hole physics and not a transformation mapping, the presented framework allows for an experimental demonstration of the GPC behavior in open quantum systems. We emphasize that because the measurement is performed on a quantum system that obeys fermion statistics, the results provide experimental evidence that supports the GPC behavior for any quantum system obeying fermion statistics including systems that are composed of either composite or fundamental fermions.

A ladder-like state preparation with multiple variables and a 1-RDM tomography, described in the Methods, is employed to explore the 1-RDM set on the quantum computer. The variables in the state preparation are sampled randomly to cover the allowed set of 1-RDMs. While m qubits are prepared in a state on the device, n of the m qubits are treated as part of the system with the remaining $m-n$ qubits representing the bath (environment). When $m=n$, the system is closed, and the GPCs of the system 1-RDM are satisfied by all randomly prepared states. When $m>n$, however, the n-qubit system is open, and the GPCs of the system 1-RDM may be violated by some of the prepared states. Demonstration of the GPC violation shows experimentally that the GPCs are only required for pure quantum states. The experiment probes one of the most fundamental relations in quantum mechanics—the Pauli exclusion principle and its generalization.

Verification of openness of a three-qubit system. For three-qubit quantum states, the 1-RDM natural occupations, obtained from measurement of the 1-RDM on the quantum computer, are shown in the Pauli polytope in Fig. 2a (and also in Supplementary Fig. 16). The obtained result is in close agreement with the findings shown by Smart et al.[23], with the majority of measured occupation sets being inside the GPC-defined region of the polytope (yellow). The simulated results (Supplementary Figs. 6 and 11) show no GPC violation, which indicates that the states in violation in Fig. 2a are a consequence of the quantum noise. Therefore, we confirm that a closed three-qubit system obeys GPCs for three fermions in six orbitals.

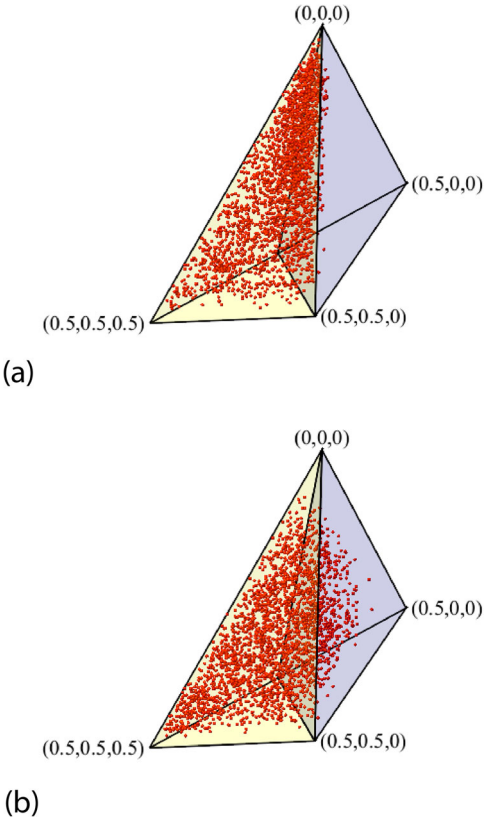

Fig. 2 Comparison of polytopes for three and four qubits. Polytopes showing the sets of three lowest natural occupations, ordered from highest to lowest, for the three-qubit system (**a**) and for the four-qubit system (**b**), measured on ibmq_jakarta. The sets of occupations lying inside the yellow region of the polytope are compatible with at least one closed (pure-state) quantum system. Sets of natural occupations that lie in the blue region of the polytope are only compatible with an open (ensemble) quantum system. Addition of a single environmental qubit to the closed three-qubit system results in the violation of the generalized Pauli constraints (GPCs) and allows the quantum system to reach openness.

To investigate the GPC behavior with an additional (environmental) qubit added to the three-qubit system, we prepared and measured four-qubit states on the quantum device. Here, the N-representability inequalities for both a system of three fermions in six orbitals (three qubits) and a system of four fermions in eight orbitals (four qubits) were examined. When the ancillary qubit is treated as an environmental qubit, the GPCs for the three-qubit system are violated (Fig. 2b), with a significant portion of the measured occupation sets being in the blue region of the polytope, defined solely by the ordinary Pauli constraints. When all four qubits are treated in the same conditions, there is no violation of the inequalities for the four-qubit system. These results, consistent in noiseless (Supplementary Fig. 7) and noisy environments (Supplementary Figs. 12 and 17), experimentally verify the sufficient condition at the level of a single particle for the openness of a many-particle quantum system, as proposed by Chakraborty and Mazziotti[22]. We show that to reach sets of occupation numbers that are only compatible with an open three-qubit quantum system, it is sufficient to add one environmental qubit to the closed three-qubit system. This demonstration of the expansion of accessible 1-RDMs provides a unique tool for determining the optimal size of the effective bath in open quantum system modeling on quantum devices.

The distributions captured for a five-qubit system in Fig. 3a–c suggest that a single ancilla qubit may also be sufficient for there

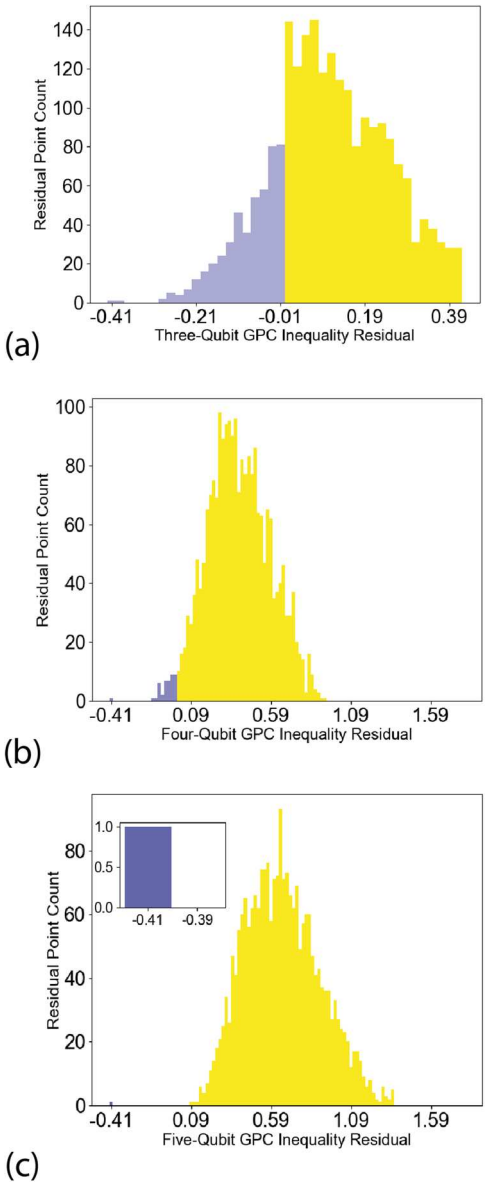

Fig. 3 Inequality residual distributions for five qubits. Bar graphs showing the distribution of higher-inequality residuals in the region defined by the generalized Pauli constraints (yellow only) and the region defined by ordinary Pauli constraints (blue and yellow) for the five-qubit system, collected on ibmq_jakarta; **a** three-qubit inequality, **b** four-qubit inequality, **c** five-qubit inequality.

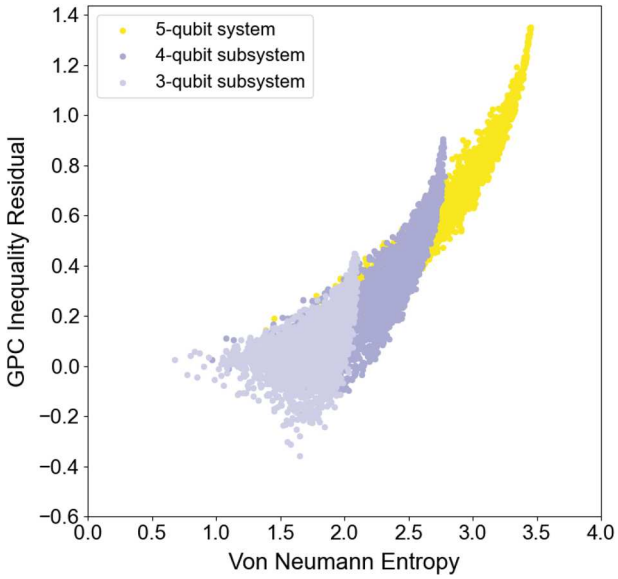

Fig. 4 Relationship between the constraints and entropy. Generalized Pauli constraints (GPCs) inequality residual plotted as a function of von Neumann entropy for the 5-qubit system and its respective, 4- and 3-qubit subsystems from occupations measured on ibmq_jakarta. Light (dark) blue points represent the subsystem where there is some amount of violation of the respective, 3-qubit (4-qubit) GPC inequality for the prepared states. Yellow points represent the total system, where there is no violation of the respective 5-qubit GPC inequality for the prepared states.

to be a violation of the four-qubit GPCs (constraints for 4 fermions in 8 orbitals) to indicate openness of the four-qubit system (Fig. 3b). Though the number of states outside the GPC-defined region is low, the system still shows evidence for the sufficient condition for openness being at the level of a single particle, even in the presence of quantum noise. Furthermore, results simulated in the noiseless environment for all studied systems show that treating one of the m qubits as the environment generates an $(m-1)$-qubit open system whose openness is detectable by the $(m-1)$-qubit GPC (Supplementary Figs. 8–10).

These findings support previous conclusions by Liebert et al.[44] on the hierarchy of generalized exclusion principle constraints and are in line with the bounds of Borland–Dennis GPCs for a mixed state considered by Hackl et al.[43]. In particular, our results demonstrate how the flexibility of higher-order inequalities for some n-qubit system exposes the lower-order inequalities in the $(m-n)$-qubit environment, where $m>n$ (Supplementary Figs. 13–15 and 18–20). This generalization goes beyond the Borland–Dennis setting and provides a method for analyzing the mixed-state GPCs in qubit systems.

To assess the connection between the GPC inequalities and the degree of entanglement in the considered systems, we analyze the GPC inequality residual as a function of von Neumann entropy[45]. Figure 4 and Supplementary Figs. 21–25 show the von Neumann entropy, generally, being minimized in the limit of high GPC violation. In addition, the results demonstrate how states in the pure-state polytope regime (yellow points in Fig. 4) can exhibit a greater mixed character in the 1-RDM than the states in the ensemble-state polytope regime (light blue points with GPC inequality residual <0 in Fig. 4). Finally, increasing entropy in the system shifts it away from the Borland–Dennis setting, which can be directly quantified in the comparison between an ideal simulation and a noisy quantum device, making this analysis a useful tool for error-mitigation purposes.

Discussion. We have experimentally verified the violation of the GPCs in an open quantum system. Specifically, we showed that the GPCs of a n-qubit system with a $(m-n)$-qubit environment where $m>n$ are generally violated. The importance of the result is that it shows that evidence of the openness of a many-fermion quantum system can be decoded from only a knowledge of the 1-RDM. In the case of the 3-qubit systems we have an intuitive, geometric picture of the violation in terms of a violation of the Borland–Dennis facet of the GPC polytope. Similarly, for higher-qubit systems the degree of the GPC violation provides a computational measure of the openness of the quantum system.

This experimental verification of the violation of GPCs due to environmental interactions has potentially important applications from quantum computing and sensing to noise-assisted energy transfer. First, they may be used for the development of efficient

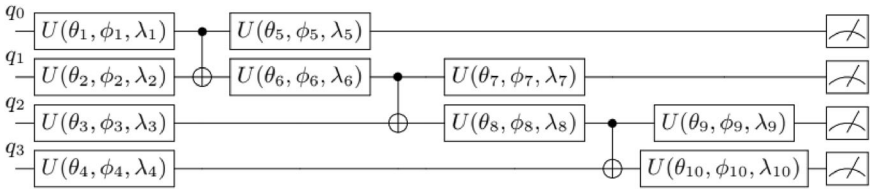

Fig. 5 Four-qubit state preparation. Quantum circuit used for the state preparation of a four-qubit system. The same logic was used for all state preparations (Supplementary Figs. 1–5).

quantum simulation algorithms for open quantum systems; for example, in combination with the density-matrix purification theory[46], they provide a framework for determining the practical size of the effective bath. Second, we observe that the 1-RDM eigenvalue sets measured on the quantum computer are consistently pulled away from the edge states, $|\mathrm{EPR}\rangle$, $|\mathrm{GHZ}\rangle$, and $|\mathrm{Slater}\rangle$, toward the inside of the GPC-defined polytope, suggesting a signature behavior of quantum noise with respect to the Pauli polytope. Considering the origins and nature of such 1-RDM behavior with respect to the GPCs has the potential to serve as a benchmarking tool for noise characterization on different quantum devices and the development of novel noise-mitigation techniques. Third, the GPCs can be used in multi-qubit quantum sensors to enhance their sensitivity over 1- or 2-qubit quantum sensors. Finally, because the violation of the GPCs enlarges the set of physically accessible 1-RDMs, it can be used to understand and predict the role of noise in assisting energy transfer.

In summary, the demonstration of GPC violation in open quantum systems on quantum devices probes one of the most fundamental relations in quantum mechanics—the Pauli exclusion principle and its generalization. While many experiments have confirmed and reconfirmed that two fermions cannot occupy the same quantum state—the Pauli exclusion principle for fermions, the present work provides an experimental demonstration of the satisfaction and violation of the pure-state generalized Pauli exclusion principle in closed and open quantum systems, respectively. Albeit a fundamental result, the GPCs are central to many-fermion and many-qubit quantum systems with potential applications for building more error-tolerant quantum computers, designing more sensitive multi-qubit quantum sensors, and harnessing the environment to enhance energy transfer in materials.

Methods

State preparation. The state preparation algorithm used in this work employs unitary rotations of control and target qubits with CNOT gates in between (Fig. 5). For a four-qubit system, this can be expressed as follows:

$$\begin{aligned}\mathbb{U}_a \;=\; & U_3(\theta_{10},\phi_{10},\lambda_{10})U_2(\theta_9,\phi_9,\lambda_9)C_2^3\\ & U_2(\theta_8,\phi_8,\lambda_8)U_1(\theta_7,\phi_7,\lambda_7)C_1^2\\ & U_1(\theta_6,\phi_6,\lambda_6)U_0(\theta_5,\phi_5,\lambda_5)C_0^1\\ & U_3(\theta_4,\phi_4,\lambda_4)U_2(\theta_3,\phi_3,\lambda_3)\\ & U_1(\theta_2,\phi_2,\lambda_2)U_0(\theta_1,\phi_1,\lambda_1)\end{aligned}$$

where U_i are unitary rotations around three Euler angles $(\theta_{i+1}, \phi_{i+1}, \lambda_{i+1})$ on qubit i. The U_3 gates are defined as follows:

$$U_3(\theta,\phi,\lambda) = \begin{bmatrix} \cos(\frac{\theta}{2}) & -e^{i\lambda}\sin(\frac{\theta}{2}) \\ e^{i\phi}\sin(\frac{\theta}{2}) & e^{i\phi+i\lambda}\cos(\frac{\theta}{2}) \end{bmatrix} \quad (5)$$

and the CNOT gates, C_i^j are standard with i control and j target qubits. The same algorithm is applied to all state preparations with additional rotations and CNOT gates added for each extra qubit in the system (see Supplementary Figs. 1–5). The many unitary rotations allow for a wide range of parameter tuning to span the entirety of the Pauli polytope. In addition, this algorithm includes some local degrees of freedom[47] and suggests that qubit-ordering dependence may be removed[23]. A total of 2050 measurements of each prepared state were made to ensure the statistical robustness of the collected data. The measurements were obtained by simulating each circuit over a range of random angles, θ, ϕ, and λ, from −180° to 180° used for the single-qubit unitary rotations of qubits, as defined above.

Quantum tomography. To directly measure the eigenvalues of the 1-RDM on a quantum device, we exploit the restriction of the N-fermions in $2N$-orbitals system to a system of N qubits, where each qubit is a two-level system sharing an electron. In the second quantization, the elements of the 1-RDM are given by

$${}^1D_j^i = \langle\psi|\hat{a}_i^\dagger\hat{a}_j|\psi\rangle, \quad (6)$$

where $\hat{a}_i^\dagger$ creates a particle in the ith orbital and $\hat{a}_j$ annihilates a particle in the jth orbital, where i and j correspond to the same qubit[35]. A one-qubit 1-RDM can be constructed as follows:

	$\hat{a}_{p,0}$	$\hat{a}_{p,1}$
$\hat{a}_{p,0}^\dagger$	$\hat{a}_{p,0}^\dagger\hat{a}_{p,0}$	$\hat{a}_{p,0}^\dagger\hat{a}_{p,1}$
$\hat{a}_{p,1}^\dagger$	$\hat{a}_{p,1}^\dagger\hat{a}_{p,0}$	$\hat{a}_{p,1}^\dagger\hat{a}_{p,1}$

for some qubit p. In the Pauli basis, these elements can be written as follows:

$$\hat{a}_{p,0}^\dagger\hat{a}_{p,0} = \begin{pmatrix}1 & 0\\ 0 & 0\end{pmatrix} = \frac{1}{2}(I + Z_p) \quad (7)$$

$$\hat{a}_{p,0}^\dagger\hat{a}_{p,1} = \begin{pmatrix}0 & 1\\ 0 & 0\end{pmatrix} = \frac{1}{2}(X_p + iY_p) \quad (8)$$

$$\hat{a}_{p,1}^\dagger\hat{a}_{p,0} = \begin{pmatrix}0 & 0\\ 1 & 0\end{pmatrix} = \frac{1}{2}(X_p - iY_p) \quad (9)$$

$$\hat{a}_{p,1}^\dagger\hat{a}_{p,1} = \begin{pmatrix}0 & 0\\ 0 & 1\end{pmatrix} = \frac{1}{2}(I - Z_p) \quad (10)$$

Since the expectations of the single-qubit Pauli matrices can be directly obtained on a quantum device, it is straightforward to obtain the expectation values of the 1-RDM elements for each state preparation.

Quantum device specifications. This work utilized superconducting-qubit IBM Quantum devices available online, ibmq_qasm_simulator, ibmq_jakarta, and a noise model qasm simulator of ibmq_jakarta (qasm_simulator(ibmq_jakarta)). ibmq_jakarta is one of the IBM Quantum Falcon Processors[37,48]. The quantum computer is composed of fixed-frequency transmon qubits with co-planar waveguide resonators[49,50]. For calibration details, see Supplementary Table 1.

Data availability

Supporting data can be found in Supplementary Figs. 1–25. Any additional data will be made available upon reasonable request.

Code availability

Code will be made available upon reasonable request.

Received: 23 January 2023; Accepted: 3 July 2023;
Published online: 17 July 2023

References

1. Pauli, W. & In, H. *Uber den Zusammenhang des Abschlusses der Elektronen-gruppen im Atom mit der Komplexstruktur der Spektren*. Tech. Rep. (1925).
2. Dirac, P. A. M. & Fowler, R. H. On the theory of quantum mechanics. *Proc. R. Soc. Lond. A* **112**, 661 (1926).

3. Heisenber, V. W. in Kopenhagen, *Mehrkrperproblem und Resonanz in der Quantenmechanik*. Tech. Rep. (1926).
4. Coleman, A. J. Structure of fermion density matrices. *Rev. Mod. Phys.* **35**, 668 (1963).
5. Borland, R. E. & Dennis, K. The conditions on the one-matrix for three-body fermion wavefunctions with one-rank equal to six. *J. Phys. B At. Mol. Opt. Phys.* **5**, 7–15 (1972).
6. Klyachko, A. A. Quantum marginal problem and N-representability. *J. Phys. Conf. Ser.* **36**, 72 (2006).
7. Altunbulak, M. & Klyachko, A. The Pauli principle revisited. *Commun. Math. Phys.* **282**, 287 (2008).
8. Schilling, C., Gross, D. & Christandl, M. Pinning of fermionic occupation numbers. *Phys. Rev. Lett.* **110**, 040404 https://pdfs.semanticscholar.org/3c9c/7391bb56738c63bc9cc7be21e5cdfeebc3c6.pdf?_ga=2.106787395.1978485703.1576770206-72123017.1576770206 (2013).
9. Chakraborty, R. & Mazziotti, D. A. Generalized Pauli conditions on the spectra of one-electron reduced density matrices of atoms and molecules. *Phys. Rev. A* **89**, 042505 https://journals.aps.org/pra/abstract/10.1103/PhysRevA.89.042505 (2014).
10. Theophilou, I., Lathiotakis, N. N., Marques, M. A. L. & Helbig, N. Generalized Pauli constraints in reduced density matrix functional theory. *J. Chem. Phys.* **142**, 154108 (2015).
11. Mazziotti, D. A. Pure-N-representability conditions of two-fermion reduced density matrices. *Phys. Rev. A* **94**, 032516 https://journals.aps.org/pra/abstract/10.1103/PhysRevA.94.032516 (2016).
12. Benavides-Riveros, C. L., Gracia-Bondía, J. M. & Springborg, M. Quasipinning and entanglement in the lithium isoelectronic series. *Phys. Rev. A* **88**, 022508 https://journals.aps.org/pra/abstract/10.1103/PhysRevA.88.022508 (2013).
13. Schilling, C. Quasipinning and its relevance for *N*-fermion quantum states. *Phys. Rev. A* **91**, 022105 (2015).
14. Schilling, C. Hubbard model: pinning of occupation numbers and role of symmetries. *Phys. Rev. B* **92**, 155149 (2015).
15. Tennie, F., Vedral, V. & Schilling, C. Influence of the fermionic exchange symmetry beyond Pauli's exclusion principle. *Phys. Rev. A* **95**, 022336 (2017).
16. Benavides-Riveros, C. L. & Springborg, M. Quasipinning and selection rules for excitations in atoms and molecules. *Phys. Rev. A* **92**, 012512 (2015).
17. Chakraborty, R. & Mazziotti, D. A. Structure of the one-electron reduced density matrix from the generalized Pauli exclusion principle. *Int. J. Quantum Chem.* **115**, 1305 (2015).
18. Chakraborty, R. & Mazziotti, D. A. Role of the generalized Pauli constraints in the quantum chemistry of excited states. *Int. J. Quantum Chem.* **116**, 784 (2016).
19. Benavides-Riveros, C. L. & Schilling, C. Natural extension of hartree-fock through extremal 1-fermion information: overview and application to the lithium atom. *Z. Phys. Chem.* **230**, 703 (2016).
20. Davies, E. *Quantum Theory of Open Systems* (Academic Press) https://books.google.com/books?id=I5kuAAAAIAAJ (1976).
21. Breuer, H. P. & Petruccione, F. *The Theory of Open Quantum Systems* (Oxford University Press, 2002).
22. Chakraborty, R. & Mazziotti, D. A. Sufficient condition for the openness of a many-electron quantum system from the violation of a generalized Pauli exclusion principle. *Phys. Rev. A* **91**, 010101 (2015).
23. Smart, S. E., Schuster, D. I. & Mazziotti, D. A. Experimental data from a quantum computer verifies the generalized Pauli exclusion principle. *Comm. Phys.* **2**, 11 (2019).
24. Barends, R. et al. Digital quantum simulation of fermionic models with a superconducting circuit. *Nat. Commun.* **6**, 7654 (2015).
25. Ma, R. et al. A dissipatively stabilized Mott insulator of photons. *Nature* **566**, 51 (2019).
26. Sager, L. M., Safaei, S. & Mazziotti, D. A. Potential coexistence of exciton and fermion-pair condensations. *Phys. Rev. B* **101**, 081107 (2020).
27. Warren, S., Sager-Smith, L. M. & Mazziotti, D. A. Quantum simulation of quantum phase transitions using the convex geometry of reduced density matrices. *Phys. Rev. A* **106**, 012434 (2022).
28. Sager, L. M. & Mazziotti, D. A. Entangled phase of simultaneous fermion and exciton condensations realized. *Phys. Rev. B* **105**, L121105 (2022).
29. Smart, S. E., Hu, Z., Kais, S. & Mazziotti, D. A. Relaxation of stationary states on a quantum computer yields a unique spectroscopic fingerprint of the computer's noise. *Comm. Phys.* **5**, 28 (2022).
30. Sager, L. M. & Mazziotti, D. A. Cooper-pair condensates with nonclassical long-range order on quantum devices. *Phys. Rev. Research* **4**, 013003 (2022).
31. Mazziotti, D. A., Smart, S. E. & Mazziotti, A. R. Quantum simulation of molecules without fermionic encoding of the wave function. *New J. Phys.* **23**, 113037 (2021).
32. Head-Marsden, K., Flick, J., Ciccarino, C. J. & Narang, P. Quantum information and algorithms for correlated quantum matter. *Chem. Rev.* **121**, 5 (2021).
33. McArdle, S., Endo, S., Aspuru-Guzik, A., Benjamin, S. C. & Yuan, X. Quantum computational chemistry. *Rev. Mod. Phys.* **92**, 015003 (2020).
34. Bian, T., Murphy, D., Xia, R., Daskin, A. & Kais, S. Quantum computing methods for electronic states of the water molecule. *Mol. Phys.* **117**, 2069 (2019).
35. Aspuru-Guzik, A., Dutoi, A. D., Love, P. J. & Head-Gordon, M. Simulated quantum computation of molecular energies. *Science* **309**, 1704 (2005).
36. Sager, L. M., Smart, S. E. & Mazziotti, D. A. Preparation of an exciton condensate of photons on a 53-qubit quantum computer. *Phys. Rev. Res.* **2**, 043205 (2020).
37. IBM-Quantum https://quantum-computing.ibm.com/ (2021).
38. Chakraborty, R. & Mazziotti, D. A. Sparsity of the wavefunction from the generalized Pauli exclusion principle. *J. Chem. Phys.* **148**, 054106 (2018).
39. Dür, W., Vidal, G. & Cirac, J. I. Three qubits can be entangled in two inequivalent ways. *Phys. Rev. A* **62**, 062314 (2000).
40. Einstein, A., Podolsky, B. & Rosen, N. Can quantum-mechanical description of physical reality be considered complete? *Phys. Rev.* **47**, 777 (1935).
41. Greenberger, D. M. GHZ (Greenberger—Horne—Zeilinger) theorem and GHZ states. In *Compendium of Quantum Physics* (eds Greenberger, D., Hentschel, K. & Weinert, F) 258–263 (Springer Berlin Heidelberg, Berlin, Heidelberg) https://doi.org/10.1007/978-3-540-70626-7_78 (2009).
42. Higuchi, A., Sudbery, A. & Szulc, J. One-qubit reduced states of a pure many-qubit state: polygon inequalities. *Phys. Rev. Lett.* **90**, 107902 (2003).
43. Hackl, L., Li, D., Akopian, N. & Christandl, M. Experimental proposal to probe the extended Pauli principle. Preprint at arXiv:2107.05961 (2021).
44. Liebert, J., Castillo, F., Labbé, J.-P. & Schilling, C. Foundation of one-particle reduced density matrix functional theory for excited states. *J. Chem. Theory Comput.* **18**, 124 (2022).
45. von Neumann, J. *Mathematical Foundations of Quantum Mechanics* (Princeton University Press) https://books.google.com/books?id=JLyCo3RO4qUC (1955).
46. Schlimgen, A. W., Head-Marsden, K., Sager-Smith, L. M., Narang, P. & Mazziotti, D. A. Quantum simulation of open quantum systems using density-matrix purification. Preprint at https://doi.org/10.48550/ARXIV.2207.07112 (2022).
47. Sudbery, A. On local invariants of pure three-qubit states. *J. Phys. A Math. and Gen.* **34**, 643 (2001).
48. Qiskit contributors. Qiskit: An open-source framework for quantum computing. https://doi.org/10.5281/zenodo.2573505 (2023).
49. Koch, J. et. al. Charge-insensitive qubit design derived from the Cooper pair box. *Phys. Rev. A* **76**, 042319 https://journals.aps.org/pra/abstract/10.1103/PhysRevA.76.042319 (2007).
50. Chow, J. M. et. al. Simple all-microwave entangling gate for fixed-frequency superconducting qubits. *Phys. Rev. Lett.* **107**, 080502 https://journals.aps.org/prl/abstract/10.1103/PhysRevLett.107.080502 (2011).

Acknowledgements

D.A.M. gratefully acknowledges NSF QuBBE Quantum Leap Challenge Institute (NSF OMA-2121044), the U.S. National Science Foundation Grants No. CHE-2155082 and CHE-2035876, and the Department of Energy, Office of Basic Energy Sciences, Grant DE-SC0019215. L.M.S. acknowledges support from the NSF Graduate Research Fellowship Program, Grant DGE-1746045. We acknowledge the use of IBM Quantum services for this work. The views expressed are those of the authors and do not reflect the official policy or position of IBM or the IBM Quantum team.

Author contributions

D.A.M. conceived of the research project. I.A., L.M.S., and D.A.M. developed the theory. I.A. performed the calculations. I.A., L.M.S., and D.A.M. discussed the data and wrote the manuscript.

Competing interests

The authors declare no competing interests.

Additional information

Supplementary information The online version contains supplementary material available at https://doi.org/10.1038/s42005-023-01295-w.

Correspondence and requests for materials should be addressed to David A. Mazziotti.

Peer review information *Communications Physics* thanks the anonymous reviewers for their contribution to the peer review of this work.